

PAPER

Metamagnetism emergence and spectroscopic elucidation of SmFeO_3 nanoceramics

To cite this article: A Paul Blessington Selvadurai *et al* 2019 *J. Phys. D: Appl. Phys.* **52** 435002

View the [article online](#) for updates and enhancements.



IOP | ebooks™

Bringing you innovative digital publishing with leading voices to create your essential collection of books in STEM research.

Start exploring the collection - download the first chapter of every title for free.

Metamagnetism emergence and spectroscopic elucidation of SmFeO₃ nanoceramics

HPSTAR
842-2019

A Paul Blessington Selvadurai^{1,6}, R Thiyagarajan², V Pazhanivelu³,
R Suriakarthick¹, Wenge Yang^{2,4}, R Murugaraj⁵ and C Venkateswaran¹

¹ Department of Nuclear Physics, University of Madras, Chennai-25, India

² Center for High Pressure Science and Technology Advanced Research (HPSTAR), Shanghai 201203, People's Republic of China

³ Beijing National Laboratory for Condensed Matter Physics, Institute of Physics, Chinese Academy of Sciences, Beijing 100190, People's Republic of China

⁴ Center for the Study of Matter at Extreme Conditions, Florida International University, Miami, FL 33199, United States of America

⁵ Department of Physics, MIT Campus, Anna University, Chennai-44, India

E-mail: paul.blessington123@gmail.com

Received 18 January 2019, revised 30 June 2019

Accepted for publication 12 July 2019

Published 8 August 2019



Abstract

Temperature- and field-dependence of magnetization measurements on SmFeO₃ nanoceramics have been carried out, and a first order type metamagnetic phase transition has been observed below 280 K. The Arrott plot on $M(H)$ measurements confirms the emergence of such a first order transition, this could be argued by the creation of a ferromagnetic cluster between the antiferromagnetic Sm³⁺-O-Fe³⁺ and Fe³⁺-O-Fe³⁺ chains by Sm³⁺ ions around the respective transition. Additionally, a quasi-paramagnetic ordering of Sm³⁺ spins is observed below 20 K due to canted moment from Sm³⁺-O-Sm³⁺. Electron paramagnetic resonance and Raman measurements at various temperatures exhibit an analogue to the instantaneous first order metamagnetic transition, confirming the predominance of Sm³⁺-O-Fe³⁺ and Fe³⁺-O-Fe³⁺ interactions above and below 273 K, respectively. The present study brings an important aspect of the presence of the magnetic property in SmFeO₃ pertaining to active and non-active interaction of Sm-O-Fe at the nanoscale regime.

Keywords: magnetic perovskite, x-ray diffraction, metamagnetism, electron paramagnetic resonances, Raman spectroscopy

(Some figures may appear in colour only in the online journal)

1. Introduction

Orthoferrites (RFeO₃; R: Rare earth elements) have gained interest among researchers due to their fascinating magneto-optic [1, 2], spin switching [3] and multiferroic properties [4–6]. Predominantly, it has an orthorhombic perovskite structure (space group: $Pbnm$) with two magnetic sublattices from 4f and 3d electrons of R³⁺ and Fe³⁺, respectively [6].

This feature leads to three complex interactions in Fe³⁺-O-Fe³⁺, R³⁺-O-Fe³⁺ and R³⁺-O-R³⁺ sublattices. The first one (Fe³⁺-O-Fe³⁺) comes into the picture fairly at high temperatures, usually in the range of 650–700 K, where the Fe-sublattice exhibits a weak ferromagnetism (FM) from the canted antiferromagnetic (AFM) spins. The second interaction (R³⁺-O-Fe³⁺) plays a crucial role in the intermediate temperature region (~80–480 K) to order the transition-metal spins resulting in a complex magnetic structure; so-called spin reorientation [7]. The third interaction (R³⁺-O-R³⁺) is at

⁶ Author to whom any correspondence should be addressed.

very low temperatures ($\sim 5\text{--}10\text{ K}$) and reveals AFM behavior through the super-exchange phenomenon [7]. These transitions could be altered by internal (chemical doping) and external perturbations, such as temperature and magnetic field to open up exotic magnetic phase transitions.

These trends were observed in a conventional orthoferrite compound SmFeO_3 through various studies. The appearance of canted G-type AFM below 680 K (T_N) leads to a weak FM component along the c axis [1, 3, 5–8]. By reducing the temperature further, magnetic and spin components of Fe^{3+} ions are aligned along the c and b axes, respectively, exactly at 480 K . This behavior leads to a spin reorientation transition with a second order nature in between 480 K and 450 K [1, 7]. Below 450 K , the axes of magnetic and spin components of Fe^{3+} ions are interchanged, and lead to a spin switching phenomenon. On further reduction in temperature, Sm^{3+} ions order at 5 K which induces a magnetization reversal. These three complex magnetic transitions (spin reorientation, spin switching and magnetization reversal) correspond to $\text{Fe}^{3+}\text{--O--Fe}^{3+}$, $\text{R}^{3+}\text{--O--Fe}^{3+}$ and $\text{R}^{3+}\text{--O--R}^{3+}$ sublattices, respectively [8–10].

SmFeO_3 nanoparticle and its size effect are reported by Ahulwat *et al* [6] and Chaturvedi *et al* [7]. They emphasize the size/surface effect of nanoparticles and magnetic interaction between Sm^{3+} and Fe^{3+} play intriguingly on the magnetic domain. It significantly influences the compensation temperature. Wang *et al* [9] reported the difference in the spin moment of Sm^{3+} and Fe^{3+} interaction in SmFeO_3 , where the cluster of active (AFM aligned between Sm^{3+} and Fe^{3+} moments) and non-active (FM aligned between Sm^{3+} and Fe^{3+} moments) interaction act as ferrimagnetic at the local scale. Fu *et al* [10] also reported a quasi-FM and AFM resonance through Sm--O--Fe interaction across 200 K and 300 K . Hence, the presence of active and non-active magnetic interactions between Sm^{3+} and Fe^{3+} can express new magnetic features in SmFeO_3 across those temperature. Here, in our report, we observed (i) a first-order metamagnetic phase transition between 250 K and 200 K , (ii) a quasi-paramagnetic ordering below 20 K , and (iii) evidence for these transitions in electron paramagnetic resonance (EPR) and Raman measurements. The present study brings an important aspect of the presence of the magnetic property in SmFeO_3 pertaining to active and non-active interaction of Sm--O--Fe at the nanoscale regime. This study evokes a spectroscopic signature for metamagnetic transitions in SmFeO_3 nanoceramics.

2. Experimental details

SmFeO_3 (SFO) nanoceramics were prepared by the citrate combustion method, where high purity chemicals of $\text{Sm}(\text{NO}_3)_2 \cdot 6\text{H}_2\text{O}$ and $\text{Fe}(\text{NO}_3)_3 \cdot 9\text{H}_2\text{O}$ were used in synthesizing SmFeO_3 nanoceramics; the detailed preparation process is reported elsewhere [2]. The quality of prepared sample was investigated using an x-ray diffractometer (XRD-Smart Lab, Rigaku) with Cu K_α radiation, and surface morphology was investigated using high-resolution scanning electron microscopy (SEM). Magnetization measurements were performed using the Physical Property Measurement System-Vibrating

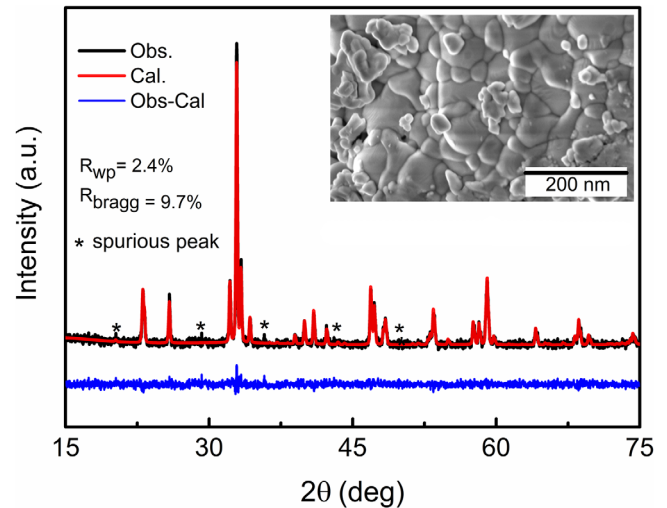


Figure 1. XRD pattern (black points) and corresponding Rietveld refinement (red line) of prepared SFO (inset: SEM micrograph of prepared SFO).

Sample Magnetometer (PPMS-VSM; Quantum Design, USA) module. Temperature dependence of magnetization [$M(T)$] was recorded upon zero-field cooling (ZFC) and field-cooling (FC) cycles with an applied magnetic field of 500 Oe in the temperature range of $300\text{--}2\text{ K}$. Field dependence of magnetization [$M(H)$] was recorded up to a field of 3 T at various temperatures. EPR and Raman spectra were recorded using the JEOL-JES FA200 and Reinshaw inVia (with the 785 nm excitation) systems in the temperature range of 433 to 153 K in steps of 40 K .

3. Results and discussion

Figure 1 shows the XRD pattern of SFO and its corresponding Rietveld refinement. The refinements suggest that the prepared sample is pure phase with the orthorhombic space group: $Pnma$. The derived structural parameters are $a = 5.4029(2)$; $b = 5.5932(2)$ and $c = 7.7141(3)\text{ \AA}$, which agree with literature reports [3, 4]. The SEM micrograph of prepared SFO is shown in the inset of figure 1, and it reveals the dense and inhomogeneous microstructure of the prepared sample.

Figure 2(a) shows the $M(T)$ of prepared SFO during ZFC and FC cycles under the magnetic field of 500 Oe in the temperature range of $300\text{--}2\text{ K}$. Near to the room temperature, $\text{Fe}^{3+}\text{--O--Fe}^{3+}$ sublattice creates a canted FM along the a axis. It dominates until $\sim 270\text{ K}$ by showing a magnetization plateau. A broad maximum peak has been observed with magnetization of $81 \times 10^{-3}\text{ emu g}^{-1}$ between 270 K and 190 K in both cycles (shown in the inset of figure 2(a)). It is a first order metamagnetic transition in this temperature region, and is explained as follows: most of the Sm^{3+} magnetic moment plays an inactive role in this temperature region, and creates weaker $\text{Sm}^{3+}\text{--O--Fe}^{3+}$ interaction, which could act as FM entities [1, 9]. On the other hand, few active Sm^{3+} moments align antiparallel with Fe^{3+} moments in the local domain and act as AFM entities. Due to the roles of active and inactive Sm^{3+} moments, the FM-AFM spin fluctuation emerges over this temperature region, which emphasizes the metamagnetism in

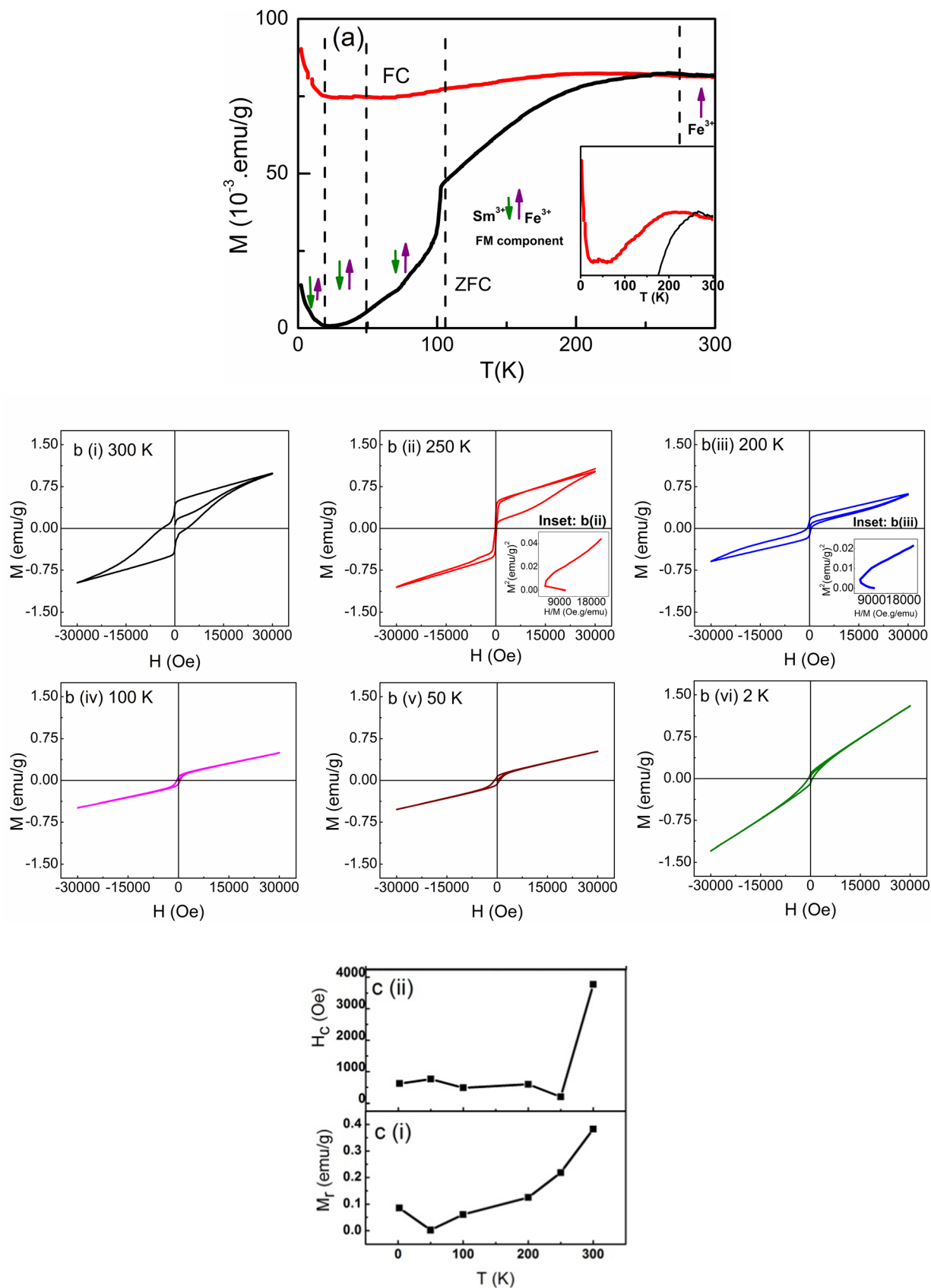


Figure 2. (a) Temperature dependence of magnetization of SFO during ZFC and FC cycles, (inset: enlarged view of FC and ZFC cycle data from main plot); ((b(i)–(vi)) field dependence of magnetization of SFO (inset: (b(ii)) and (b(iii)) shows the Arrott plot for 250 K and 200 K and (c(i) and (ii)) magnetic parameters M_r and H_c at various temperatures).

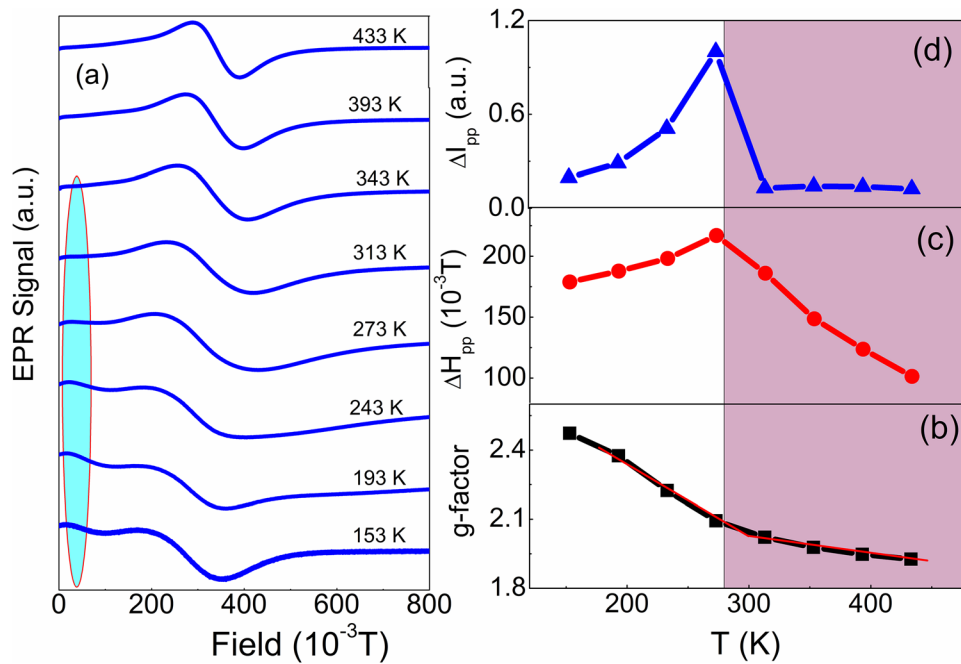


Figure 3. (a) EPR spectra of prepared SFO at various temperatures; (b) g -factor, (c) ΔH_{pp} -peak-peak width and (d) ΔI_{pp} -peak-peak intensity as function of temperature.

SFO. Several FM metals have exhibited such a behavior due to the competing interaction of FM-AFM spin-fluctuations [11].

Reducing the temperature below 190 K, magnetization decreases gradually until 20 K during the ZFC cycle, and this feature could be explained as follows: Fe^{3+} ions retain their FM component along the a direction, whereas Sm^{3+} ions exhibit FM ordering along the $-a$ axis. Hence, both of these FM behaviors cancel each other out. However, Sm^{3+} ions additionally exhibit AFM ordering along the b axes. This complete scenario creates a frustrated magnetic behavior, and decreases magnetization to almost zero while reducing the temperature to 20 K [1, 3, 5–8]. An abrupt rise in ZFC magnetization at 100 K denotes a spin switching transition, i.e. quasi discontinuous at a lower temperature. This quasi discontinuous spin switching nature cues to the native role of grain size and polycrystalline nature of the sample. On the other hand, the FC cycle maintains magnetization around $75 \times 10^{-3} \text{ emu g}^{-1}$ at 20 K. These two contradictory features between ZFC and FC cycles create a strong bifurcation and irreversibility, thereby leading to discontinuous first order transition below 225 K. While reducing the temperature below 20 K during both cycles, canted FM interaction between $\text{Sm}^{3+}\text{-O-Sm}^{3+}$ creates a quasi-paramagnetic (QPM) ordering. This kind of a low temperature QPM phenomenon is reported in $\alpha\text{-Fe}_2\text{O}_3$ [12].

Figures 2(b(i)–(vi)) show $M(H)$ of SFO up to 3 T at the temperatures of 300, 250, 200, 100, 50 and 2 K, respectively. Figure 2(b(i)) shows a broad hysteresis loop which confirms canted FM around 300 K. The appearance of S-type behavior with hysteresis in $M(H)$ at 250 and 200 K suggests a metamagnetic transition. This is due to the FM component of the inactive $\text{Sm}^{3+}\text{-O-Fe}^{3+}$ moments, switching with respect to the applied field along with the canted FM nature of the $\text{Fe}^{3+}\text{-O-Fe}^{3+}$ sublattice [1]. As temperature decreases, the interaction coupling between the Sm^{3+} and Fe^{3+} becomes

significant, thereby the AFM ordering of $\text{Sm}^{3+}\text{-O-Fe}^{3+}$ becomes dominant and thus the switching field gets shifted towards a higher field, as observed in the initial curve of $M(H)$ of 100 and 50 K, respectively. The negative slopes in the very low field regions of the Arrott plot in the insets of figures 2(b(ii) and (iii)) confirm the metamagnetic transition to be of first order. The FM component of inactive $\text{Sm}^{3+}\text{-O-Fe}^{3+}$ moments ensure a transition between 190 and 280 K, and the overlapping AFM component is dominated below and above these temperatures. $M(H)$ at 250 K and 200 K delineates the transition as shown in the Arrott plots. The $M(H)$ hysteresis at 300 K becomes wide-open, as the thermal energy weakens the FM ordering of $\text{Sm}^{3+}\text{-O-Fe}^{3+}$ ions, where the canted FM ascribed to $\text{Fe}^{3+}\text{-O-Fe}^{3+}$ interaction becomes dominant. Further, on reducing the temperature from 300 to 50 K, the $M(H)$ hysteresis apparently reduces due to the emergence of magnetic multi-domains favored by the AFM magnetic interactions. The magnetic interaction between various lattices could be analyzed by the following parameters namely remnant magnetization (M_r) and coercivity (H_c), which could be estimated from the $M(H)$ plots. The estimated values of M_r , and H_c of SFO as a function of temperature are shown in figures 2(c(i) and (ii)), respectively. As the antiparallel FM of Sm^{3+} ion compensates the FM component of Fe^{3+} ion by reducing temperature, M_r and H_c decrease (figures 2(c(i) and (ii)). The observed magnetic phenomenon ‘metamagnetism’ is also significantly manipulated by the grain size effect. As our prepared SFO is in the nanoscale regime, the reduced grain size enhances the surface effect which additionally establishes a core-shell (AFM-FM) magnetic interaction in it. This grain size effect plays a typical role on the magnetic behavior of this system [6, 7].

EPR aids in discerning the effects of $\text{Fe}^{3+}\text{-O-Fe}^{3+}$ and $\text{Sm}^{3+}\text{-O-Fe}^{3+}$ interactions, and it is shown in figure 3(a). The

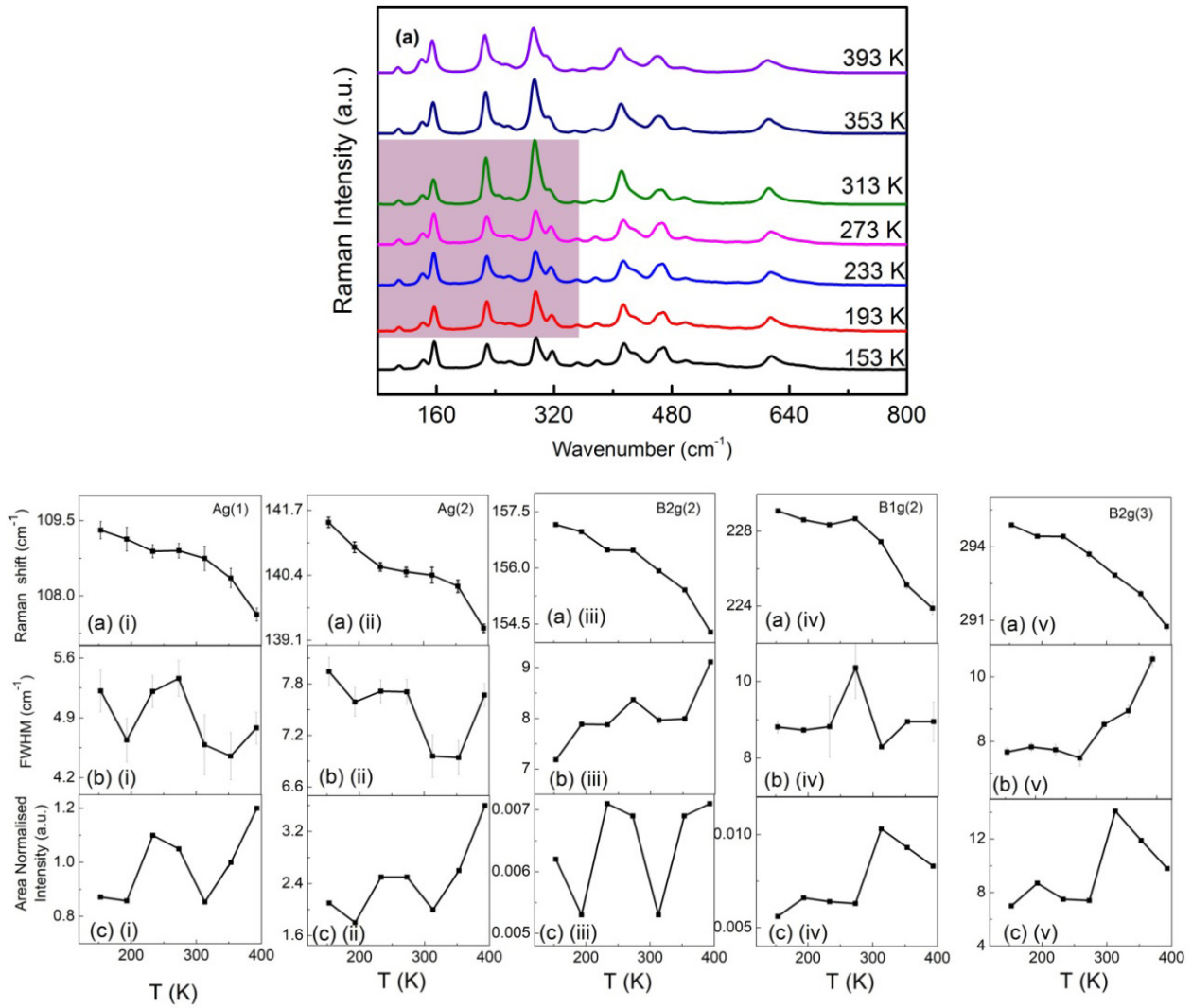


Figure 4. (a) Temperature variable SFO Raman spectra, highlighting a distinct change of Raman spectra: (a)(i)–(v) Raman shift, (b)(i)–(v) FWHM, (c)(i)–(v) intensity for some of the SFO Raman modes.

derivable parameters from EPR data such as g -factor, ΔH_{pp} –peak–peak width and ΔI_{pp} –peak–peak intensity from the EPR spectra at temperatures between 153 K and 433 K for SFO are shown in figures 3(b)–(d), respectively. The g factor of 2.021 at 313 K and above is consistent with the report, which solely depends on the Fe^{3+} ion (figure 3(a)) [13]. Further, figure 3(a) itself demonstrates a noticeable increase in the g -factor value with two distinct slopes across the measured temperature range, a corresponding change in the ΔH_{pp} and ΔI_{pp} at 313 K. Such a change is synonymous to the magnetic fluctuation [14]. It is due to the fact that Sm^{3+} and Fe^{3+} interacts with the applied field differently, and hence it could be in two different modes such as active and inactive. At 313 K, the effective magnetic moment of Sm^{3+} alone gets significantly aligned along the applied field for FM ordering, whereas $\text{Fe}^{3+}\text{--O--Fe}^{3+}$ interaction retains its canted AFM ordering. Therefore, the inactive $\text{Sm}^{3+}\text{--O--Fe}^{3+}$ interaction is involved at 313 K, and promotes a FM cluster at 313 K. This inference of FM ordering is very evident through the EPR spectra profile, where, below 313 K, the profile reveals an abrupt

change imitating a ferromagnetic resonance (FMR) signal, with a FM cluster signal at $\sim 18\text{--}15$ mT (highlighted in the oblate circle). Apparent evidence of the fact that FM ordering is lucid with the representation of normalized ΔI_{pp} is illustrated in figure 3(d), since ΔI_{pp} directly represents the spin susceptibility of the SFO system. The discontinuous change in the region from 313 K to 273 K in figure 3(d) elucidates that the increased magnetic spin contribution at 273 K and below arises from the FM component of Sm^{3+} ions rather than from the Fe^{3+} moment, as $\text{Fe}^{3+}\text{--O--Fe}^{3+}$ AFM transition and their canted moment remains rugged even at high temperature. At 153 K, the FMR signal is suppressed and also the rapid decline of ΔI_{pp} below 273 K infers the increasing antiparallel AFM ordering of $\text{Sm}^{3+}\text{--O--Fe}^{3+}$ [8].

In addition, ΔH_{pp} is inversely proportional to the spin relaxation time τ of the interacting magnetic ions. By reducing the temperature, τ is expected to increase. In the case of orthoferrites and magnetites, dipolar and exchange interactions eventually alter τ , where the superexchange narrows the line-width and the dipolar broadens it [14, 15]. Between 153 and 273 K,

the active $\text{Sm}^{3+}\text{-O-Fe}^{3+}$ AFM interaction weakens, and the inactive $\text{Sm}^{3+}\text{-O-Fe}^{3+}$ moment enhances the dipolar interaction due to their FM contribution. With a further increase in temperature the dipolar interaction weakens and $\text{Fe}^{3+}\text{-O-Fe}^{3+}$ superexchange interaction becomes dominant. Thus, the parameter ΔH_{pp} (figure 3(c)) has an ascent and descent below and above 273 K, respectively. In corroboration with the magnetic study, EPR elucidates that the AFM-FM transition, i.e. the field induced first order type metamagnetic transition between 200 and 250 K in $M(H)$ of SFO nanoceramics, is ascribed to the inactive $\text{Sm}^{3+}\text{-O-Fe}^{3+}$ interaction inducing FM cluster amidst the AFM interaction.

Unpolarised Raman spectra of SFO have been recorded under various temperatures from 153 to 393 K in steps of 40 K, and are shown in figure 4(a). SFO shows non-polar vibrational modes of $\text{Ag}(1)$, $\text{Ag}(2)$, $\text{B}_2\text{g}(2)$, $\text{B}_1\text{g}(2)$, $\text{B}_2\text{g}(3)$, $\text{Ag}(4)$, $\text{B}_1\text{g}(4)$, $\text{Ag}(7)$ and $\text{B}_2\text{g}(7)$ at 108 cm^{-1} , 140 cm^{-1} , 155 cm^{-1} , 227 cm^{-1} , 290 cm^{-1} , 317 cm^{-1} , 412 cm^{-1} , 465 cm^{-1} and 613 cm^{-1} respectively, and these values are also in good agreement with earlier reports [5, 8, 16]. Raman modes below 320 cm^{-1} schematically represent the role of Sm^{3+} ion, and it underwent a systematic change by increasing the temperature from 193 K to 313 K (highlighted area in figure 4(a)). This feature ensures that Sm^{3+} ion has an important role in magnetic ordering at 273 K which clearly coheres with the EPR and magnetization results. Any anomaly correlated to structural and/or physical properties are apparently exposed in the phonon parameters of Raman modes, such as position, full width half maximum (FWHM) and intensity of each peak. These parameters for Raman modes below 320 cm^{-1} are estimated, and shown in separate panels in figures 4(a) (i)–(v)–(c)(i)–(v). These figures vividly reveal that FWHM and intensity of these modes are subjected to more changes by increasing the temperature rather than the position, and suggest that there is no change in the volume of the sample due to magnetostriction [17]. On the other hand, it was reported in magnetic perovskites, such as RCrO_3 , rare earth magnetites, and BiFeO_3 [17–19] that any subtle magnetic interaction or transition over the temperature will influence the FWHM and intensity of Raman modes. Hence, the anomaly exists in FWHM and intensity of SFO near 273 K which unambiguously corresponds to the magnetic order transition in SFO between $\text{Sm}^{3+}\text{-O-Fe}^{3+}$ and $\text{Fe}^{3+}\text{-O-Fe}^{3+}$ interactions. The Raman spectra across the investigated temperature also reveal that it has no sign of structural phase transition.

In conclusion, SFO nanoceramics exhibit a metamagnetic transition as a result of FM-AFM fluctuation emerging between 190 K and 280 K with a broad maxima in the temperature dependence of magnetization and with a critical field transition in the magnetization. The observed metamagnetic transition is of first-order type. EPR and Raman spectroscopy studies validate the emerging transitions as due to the complex magnetic interaction across the measured temperature range. Amidst those complex interactions, the inactive Sm^{3+} ions initiate weak FM clusters to induce metamagnetism in SFO nanoceramics.

Acknowledgment

The corresponding author, Dr A Paul Blessington Selvadurai thanks DST-SERB, Govt. of India for supporting through National post-doctoral fellowship: PDF/2016/003421, and also thanks SAIF-IIT Bombay and CIF PU for EPR and Raman measurements.

ORCID iDs

A Paul Blessington Selvadurai  <https://orcid.org/0000-0002-3758-8341>

R Murugaraj  <https://orcid.org/0000-0002-8118-5478>

C Venkateswaran  <https://orcid.org/0000-0001-5627-1801>

References

- [1] De C, Nayak A K, Nicklas M and Sundaresan A 2017 Magnetic compensation-induced sign reversal of exchange bias in a multi-glass perovskite SmFeO_3 *Appl. Phys. Lett.* **111** 182403
- [2] Paul Blessington Selvadurai A, Pazhanivelu V, Jagadeeshwaran C and Murugaraj R 2015 Panneer muthuselvan, influence of Cr substitution on structural, magnetic and electrical conductivity spectra of LaFeO_3 *J. Alloys Compd.* **646** 924–930
- [3] Cao S, Zhao H, Kang B, Zhang J and Ren W 2015 Temperature induced Spin Switching in SmFeO_3 single crystal *Sci. Rep.* **4** 5960
- [4] Zhao H, Cao S, Huang R, Ren W, Yuan S, Kang B, Lu B and Zhang J 2013 Enhanced $4f$ - $3d$ interaction by Ti-doping on the magnetic properties of perovskite $\text{SmFe}_{1-x}\text{Ti}_x\text{O}_3$ *J. Appl. Phys.* **114** 113907
- [5] Chaturvedi S, Shyam P, Apte A, Kumar J, Bhattacharyya A, Awasthi A M and Kulkarni S 2016 Dynamics of electron density, spin-phonon coupling, and dielectric properties of SmFeO_3 nanoparticles at the spin-reorientation temperature: role of exchange striction *Phys. Rev. B* **93** 1–12
- [6] Ahlawat A, Kushwaha S, Khan A A, Satapathy S, Choudhary R J and Karnal A K 2017 Influence of particle size on spin switching properties and magnetoelectric coupling in SmFeO_3 *J. Mater. Sci. Mater. Electron.* **29** 927–34
- [7] Chaturvedi S, Shyam P, Bag R, Shirolkar M M, Kumar J, Kaur H, Singh S, Awasthi A M and Kulkarni S 2017 Nanosize effect: Enhanced compensation temperature and existence of magnetodielectric coupling in SmFeO_3 *Phys. Rev. B* **96** 1–13
- [8] Weber M C, Guennou M, Zhao H and Rui J 2016 Raman spectroscopy of rare-earth orthoferrites RFeO_3 ($R = \text{La}, \text{Sm}, \text{Eu}, \text{Gd}, \text{Tb}, \text{Dy}$) *Phys. Rev. B* **94** 214103
- [9] Wang X, Cheng X, Gao S, Song J, Ruan K and Li X 2016 Room temperature exchange bias in SmFeO_3 single crystal *J. Magn. Magn. Mater.* **399** 170–4
- [10] Fu X, Zeng X, Wang D, Zhang H C, Han J and Cui T J 2015 Ultralow temperature terahertz magnetic thermodynamics of perovskite-like SmFeO_3 ceramic *Sci. Rep.* **4** 14777
- [11] Punnoose A and Hays J 2005 Possible metamagnetic origin of ferromagnetism in transition-metal-doped SnO_2 *J. Appl. Phys.* **97** 10D321
- [12] Bhowmik R N, Vijayasaria G and Sinha A K 2016 Study of magnetic field induced spin order in diluted antiferromagnetic states in a Ga doped $\alpha\text{-Fe}_2\text{O}_3$ system prepared by a chemical route and air annealing *RSC Adv.* **6** 112960

- [13] Paul Blessington Selvadurai A, Pazhanivelu V, Jagadeeshwaran C, Murugaraj R, Mohammed Gazzali P M and Chandrasekaran G 2017 An analysis on structural and magnetic properties of $\text{La}_{1-x}\text{RE}_x\text{FeO}_3$ ($x = 0.0$ and 0.5 , RE = Nd, Sm and Gd) nanoparticles *Appl. Phys. A* **123** 1–11
- [14] Mall A K, Dixit A and Gupta A G R 2017 Temperature dependent electron paramagnetic resonance study on magnetoelectric YCrO_3 *J. Phys.: Condens. Matter* **29** 495805
- [15] Martin L O, Chapman J P, Lezama L, Garitaonandia J J S, Marcos J S, Rodríguez-Fernández J, Arriortuac M I and Rojo T 2006 Spin-glass behaviour in the double perovskite ' $\text{Sr}_2\text{FeTeO}_6$ ' due to mis-site disorder and cation vacancy formation *J. Mater. Chem.* **16** 66–76
- [16] Tyagi S, Sathe V G, Sharma G, Gupta M K and Poswal H K 2018 Detail investigations of SmFeO_3 under extreme condition *Mater. Chem. Phys.* **215** 393–403
- [17] Bhadram V S, Rajeswaran B, Sundaresan A and Narayan C 2013 Spin-phonon coupling in multiferroic RCrO_3 (R-Y, Lu, Gd, Eu, Sm): a Raman study *EPL* **101** 17008
- [18] Chen X *et al* 2015 Study of spin-ordering and spinreorientation transitions in hexagonal manganites through Raman spectroscopy *Sci. Rep.* **5** 13366
- [19] Singh M K, Katiyar R S and Scott J F 2008 New magnetic phase transitions in BiFeO_3 *J. Phys.: Condens. Matter* **20** 252203